

1 Deposition in the Kuznetsk Basin, Siberia: insights into the
2 Permian-Triassic transition and the Mesozoic evolution of Central Asia

3

4 Clare Davies^{a,*}, Mark B. Allen^b, Misha M. Buslov^c, Inna Safonova^c

5 ^a *Woodside Energy Ltd. Woodside Plaza, 240 St Georges Terrace, Perth, Western Australia*
6 *6000, Australia*

7 ^b *Department of Earth Sciences, University of Durham, Durham, DH1 3LE, UK*

8 ^c *Institute of Geology and Mineralogy, Russian Academy of Sciences, Siberian Branch,*
9 *Novosibirsk, Russia*

10 * Clare.Davies@woodside.com.au

11

12 ABSTRACT

13 This paper describes the Permian-Mesozoic stratigraphy of the Kuznetsk Basin, southern
14 Siberia, which is adjacent to the vast and hydrocarbon-rich West Siberian Basin and on the
15 edge of the Siberian flood basalts. The basin fill is Permian to Cretaceous in age, and is
16 dominated by non-marine siliciclastics up to ~7 km thick. Palaeocurrent indicators show
17 dominant flow to the north/northeast during the Permian to Jurassic. Fourteen lithofacies are
18 grouped in three facies associations: fluvial channel-belt, overbank and floodplain/floodplain
19 pond. Coal-bearing Permian siliciclastics are interpreted as meandering river deposits in a
20 foreland basin, with subsidence generated by thrust-sheet loading from at least three basin
21 margins. These sediments pass abruptly but conformably upwards into coal-barren sandstones
22 and conglomerates and siltstones, interpreted as braided river deposits. Two basalt flows
23 occur within the coal-barren succession. A recently-published, precise Ar-Ar age of $250.3 \pm$
24 0.7 Ma for the lower of these basalts, <50 m above the sedimentary transition, suggests that

25 the Permian-Triassic boundary occurs just above this flow. We relate the loss of coal-
26 producing flora and the increase in mean sediment grain size to vegetation loss, in turn
27 triggered by the eruption of the Siberian flood basalts to the north. End-Permian and Lower
28 Triassic(?) strata are overlain by Lower Jurassic fluvial siliciclastics via a gentle angular
29 unconformity. Conglomerates punctuate a sandstone-dominated succession that continues in
30 to the Middle Jurassic. Both the basal unconformity and the rejuvenation in sedimentation
31 may result from intracontinental thrusting at the basin margins and beyond; this thrusting was
32 triggered by orogenies at the Eurasian margin. Lower and mid Cretaceous siliciclastics are
33 poorly exposed and crop out only locally: field relations indicate an angular unconformity at
34 their base. The end-Permian stratigraphy in the Kuznetsk Basin documents the environmental
35 crisis at the time of the Siberian flood basalts, and reinforces the link between these eruptions
36 and climatic and environmental deterioration. The Mesozoic sedimentary record highlights
37 how episodic deformation influenced sediment supply to the West Siberian Basin, and is an
38 example of the record of Eurasian assembly and deformation preserved within the continental
39 interior.

40

41 *Keywords:* Permian-Triassic transition, Jurassic, Siberia, Central Asia, fluvial

42

43 **1. Introduction**

44 This paper concerns the sedimentary fill of the Permian-Cretaceous Kuznetsk Basin
45 (Kuzbass) in southern Siberia, Russia (Fig. 1). The study has three main implications, beyond
46 the basin itself. 1) The geology includes examples of sedimentation at the Permian-Triassic
47 transition, in an area affected by Siberian trap volcanism – itself held responsible for the mass
48 extinction between the Permian and Triassic (Wignall, 2001 and references therein). 2)
49 Sediment pulses, folds and unconformities within the Kuznetsk Basin are a record of tectonic

50 events during the Permian-Mesozoic evolution that affected a much wider area of Central
51 Asia. 3). Part of our observations is that north-flowing palaeo-drainage systems in the
52 Kuznetsk Basin formed part of the sediment transport system for the nearby West Siberian
53 Basin (area $>2 \times 10^6 \text{ km}^2$) and so give insights into its evolution and likely basin fill. The
54 West Siberian Basin has economic as well as academic importance, as it is one of the world's
55 main hydrocarbon producing areas (Peterson and Clarke, 1991; Vyssotski et al., 2006).

56 Our approach is to describe the regional geology first, then to document the Permian-
57 Mesozoic stratigraphy (mainly from our fieldwork in open cast coal mines, quarries and road
58 and river sections; other natural exposures are rare) and then to discuss the implications of the
59 stratigraphy for each of the three lines of study listed above.

60

61 **2. Geological background**

62

63 *2.1. Regional geology*

64 The Kuznetsk Basin has an area of 20,000 km², and is located ~300 km to the south of
65 the West Siberian Basin, and east of Novosibirsk (Fig. 1). The basin is bordered on all four
66 margins by fold and thrust belts and shear zones that deform Palaeozoic rocks and generally
67 verge towards the basin interior (Fig. 2). From the north, clockwise, these are the Tom'-
68 Kolyvan, the Kuznetsk Alatau, the Western Sayan/Gorny Altai and the Salair Range. All four
69 regions form part of the vast Altaid collage, which is the orogenic belt that constructed much
70 of the basement of Central Asia during the Palaeozoic (Şengör and Natal'in, 1996; Buslov et
71 al., 2004). Many of the Palaeozoic units are volcanic, volcanoclastic, or immature
72 siliciclastics derived from these protoliths. The unexposed and undrilled basement to the
73 basin presumably consists of similar rocks. In contrast, the Carboniferous succession is
74 carbonate-dominated, where exposed along much of the Kuznetsk Basin margin. These

75 carbonates form part of a widespread Upper Devonian - Carboniferous platform across
76 southern Central Asia (e.g. Cook et al., 1995; Gutak et al., 2008): no distinct Kuznetsk Basin
77 was present at this time. The Carboniferous carbonates pass conformably upwards into an
78 Upper Carboniferous - Permian non-marine clastic succession.

79 The exposed fill of the Kuznetsk Basin is mainly Permian in age (Fig. 2), and consists
80 of up to 5 km of Permian non-marine siliciclastics. These are notable for the coal seams they
81 contain: the Kuznetsk Basin is one of Russia's main coal-producing areas. Production is
82 largely from open cast mines, creating superb exposures of the Permian succession, and, in
83 places, overlying Mesozoic strata.

84 Geological maps show the Triassic as everywhere conformable onto the Permian
85 (Kurtigeshev et al., 2008; Lavrenov et al., 2008), with a mapped thickness in the order of
86 hundreds of metres, and including at least two basalt units (probably both lavas, several
87 metres thick, although some Russian geologists believe they are sills). Recent Ar-Ar
88 determinations on these basalts (Reichow et al., 2009) give precise ages of 250.3 ± 0.7 Ma and
89 250.7 ± 0.6 Ma, placing them and the adjacent sediments most likely in the latest Permian: the
90 Permian-Triassic boundary at the global section and stratotype at Meishan, China, lies
91 between tuffs dated at 249.25 ± 0.14 Ma and 249.83 ± 0.15 Ma (Renne et al., 1995; Reichow
92 et al., 2009). This makes it uncertain exactly where the Permian-Triassic boundary lies in the
93 Kuznetsk Basin succession, and what thickness of Triassic strata is present below the Jurassic
94 succession. The uppermost coal seam lies below these basalts, therefore for simplicity we
95 refer to the rocks previously mapped as Triassic as the end-Permian/Triassic succession,
96 allowing that the rocks above the basalts probably include some Permian deposits. However,
97 biostratigraphic frameworks for the Kuznetsk Basin conventionally place the Permian-Triassic
98 boundary at the top of the coaliferous deposits (Mogutcheva and Krugovykh, 2009), based on
99 changes in floral, ostracode, conchostracan, bivalve and charophyte assemblages.

100 The Jurassic succession overlies the Permian (and any Triassic, if present) with a
101 gentle angular unconformity (Fig. 2). The total succession is nowhere more than ~1000 m
102 thick, comprising non-marine siliciclastics, mainly of Early Jurassic age. The upper part of the
103 succession is mapped as Middle Jurassic (Buslov et al., 2007), but the non-marine nature of
104 the rocks makes precise age determinations difficult. Lower Cretaceous strata are only present
105 in the southwest of the Kuznetsk Basin and in small, somewhat speculative outliers in the
106 basin interior. There are no Late Cretaceous or Paleogene strata preserved in the basin,
107 consistent with much of Central Asia being a peneplain through this time (Allen et al., 2001).

108 All the Mesozoic strata are folded to some degree, although nowhere mapped as
109 faulted. At present the basin is being incised, and lateral shifts in drainage imply gentle, active
110 deformation, interpreted as a long-distance effect of the India-Asia collision (Allen and
111 Davies, 2007).

112

113 2.2. *Stratigraphy and age determinations*

114 There is a long history of stratigraphic study and mapping in the Kuznetsk Basin
115 (Yavorskiy and Butov, 1927; Usov, 1937) that continues to this day (Kurtigeshev et al., 2008;
116 Lavrenov et al., 2008; Mogutcheva and Krugovykh (2009). Fig. 3 summarises the
117 stratigraphic units; Fig. 4 is a summary log of the strata. The standard Russian division is the
118 suite, which is roughly equivalent to the formation of international usage. Suites carry a
119 connotation of time, as well as lithological equivalence. Two or more suites may be grouped
120 to form a series.

121 The following summary and Fig. 3 are adopted from the review in Buslov et al.
122 (2007). The Balakhonskaya Series spans the Carboniferous-Permian boundary and is the
123 oldest suite of the Kuznetsk Basin proper. It is sub-divided in to three suites: Ostrogskaya,
124 Nizhnebalakhonskaya (Lower Balakhonskaya) and Verkhnebalakhonskaya (Upper

125 Balakhonskaya). The Ostrogsкая Suite begins with a thin basal conglomerate, but is
126 apparently conformable over underlying strata in the basin interior. The unit is thinner towards
127 the west and east and absent in the north of the basin. The Nizhnebalakhonskaya Suite is the
128 lowermost coal-producing unit in the basin. In general, the coal-bearing suites begin with
129 coal-free successions which become coal-bearing with thicker seams up-section. The overlying
130 Verkhnebalakhonskaya Suite is sub-divided into four sub-suites, from bottom to top
131 Promezhutochnaya, Ishanovskaya, Kemerovskaya and Usyatskaya. Esaulova (1997) placed
132 the international Lower-Upper Permian boundary (base of the Ufimian Stage) at the base of
133 the Usyatskaya Sub-suite, which is slightly different from the scheme used by others (Buslov
134 et al., 2007). Note that Russian stratigraphic nomenclature includes a formal Middle Permian
135 division. The Kemerovskaya and Usyatskaya sub-suites include coal seams 20-30 m thick.
136 The Kolchuginskaya Series overlies the Verkhnebalakhonskaya Suite conformably, and is
137 taken to represent a second major cycle within the coal-bearing succession. It is sub-divided into
138 three suites, the oldest of which, the Kuznetskaya Suite, contains fewer coals and more
139 coarse siliciclastics than the overlying Il'inskaya and Yerunakovskaya suites.

140 Triassic strata are conventionally defined as the Lower-Middle Triassic Abinskaya
141 Series (sub-divided into the Mal'tsevskaya, Sosnovskaya and Yaminskaya suites), with the
142 Permo-Triassic boundary located at the transition from coal-bearing to coal-barren strata
143 (Mogutcheva and Krugovykh, 2009). As noted above, a basalt flow within the lower part of
144 these rocks is most likely to be end-Permian (Reichow et al., 2009), such that the Permian-
145 Triassic boundary must lie at an unknown point higher within the coal-barren succession (Fig.
146 4). These end-Permian/Triassic strata are also non-marine, making correlation difficult. The
147 upper unit (Yaminskaya Suite) is placed in the Middle Triassic.

148 Jurassic strata are grouped as the Tarbaganskaya Series, sub-divided into the
149 Rapsadskaya, Abashevskaya and Osinovskaya suites (Lower Jurassic) and the Tersyukskaya

150 Suite (Middle Jurassic, possibly Toarcian and Aalenian; Mogutcheva, 2009). Although
151 dominated by sandstones and conglomerates, the Jurassic succession also includes coals in all
152 four suites. Age determinations and regional correlations are done largely on the basis of
153 palynology (Mogutcheva, 2009). A thin (>50 m) Cretaceous succession is present in the
154 southwest of the Kuznetsk Basin (Fig. 2), where it directly overlies the Carboniferous and
155 Devonian rocks. The age range is uncertain; it is mapped as Lower and mid Cretaceous, and
156 supposed to be marine. As only one, poor-quality, outcrop was observed during fieldwork the
157 depositional environment is not analysed in any detail in this paper.

158

159

160 **3. Sedimentology of Permian and Mesozoic strata**

161

162 *3.1. Facies associations*

163 Fourteen lithofacies have been identified within the Permian-Mesozoic succession of
164 the Kuznetsk Basin and are summarised in Table 1 (with the majority illustrated in Fig. 5).
165 Localities are shown on Fig. 2, and latitudes and longitudes for each locality are given in
166 Table 2. Representative logs are shown in Figs. 6A-F (arranged in ascending stratigraphic
167 order). The lithofacies form three recurring facies associations, which are interpreted as
168 representing different fluvial environments. A summary of the three facies associations is
169 given below.

170 *3.1.1. Fluvial channel belt facies association*

171 This facies association includes facies with the following lithologies: parallel
172 laminated sandstone, trough cross-bedded sandstone, planar cross-stratified sandstone, ripple
173 cross-stratified sandstone, massive sandstone, massive conglomerate and planar cross-
174 stratified conglomerate (respectively Sl, St, Sp, Sr, Sm, Gm and Gp in Table 1). It comprises

175 planar and trough cross-stratified, very fine to coarse grained sandstones, and clast and matrix
176 supported conglomerates (Fig. 5F-I). The sandstones generally occur in sets of 0.5-1 m scale
177 with either a flat base where they overly coal (due to the resistant nature of peat to erosion
178 (McCabe, 1984; Collinson, 1996) or a scoured base and pebble lags where the underlying unit
179 is siliciclastic in origin (Figs. 6A and 6F). The fluvial systems were channelised. Individual
180 fluvial sand bodies are commonly stacked and amalgamated, forming laterally extensive,
181 uniformly thick (up to 20 m) sandstone units. The conglomerates, commonly clast
182 supported, contain rounded to subrounded clasts of 0.5-10 cm, maximum 60 cm in diameter.
183 Conglomerate beds can be single or amalgamated events from 1-10 m thick (maximum 20 m
184 thick) and internally contain foresets (Fig. 5I).

185 Permian sandstones commonly contain preserved foresets (0.5-1 m) whose scale
186 suggests initial large dune bedforms in the order of 3-5 m in height (Leclair *et al.*, 1997;
187 Ashley, 1990). This indicates channels in the order of 18-50 m deep (Bridge, 2003). Stacked,
188 laterally extensive uniformly thick sandstones are interbedded with the coal seams in the
189 coal-bearing Permian succession (Figs. 5G, 5H and 6B). The presence of several examples of
190 large-scale, 6-10 m high, sandstone sets indicates lateral bar migration of large in-channel
191 barforms, either bank attached or mid channel bars.

192 End-Permian/Triassic cross-stratified, fine-grained sandstones were deposited in 50-80
193 cm high foresets (locality S-14; Fig. 6C). These can be estimated to have formed as medium-
194 large scale dune bedforms, 1.5-3 m in height (Leclair *et al.*, 1997; Ashley, 1990) infilling
195 channels 9-30 m in depth (Bridge, 2003).

196 Jurassic sandstones were deposited in 15-20 cm high foresets estimated to have
197 formed small-medium dune barforms 60-80 cm in height (Leclair *et al.*, 1997; Ashley, 1990)
198 infilling channels in the order of 3.5-8 m deep (Bridge, 2003) to form massive to cross-
199 stratified and parallel laminated sandstone bodies (Fig. 6D).

200 Evidence for high energy sediment transport and high sediment supply comes from the
201 large scale dune bedforms, coupled with the substantial clast sizes within this facies
202 association. These features suggest a mixed and bedload transported material in high energy
203 braided fluvial (to possible meandering) system across an extensive floodplain.

204 *3.1.2. Overbank facies association*

205 This facies association is composed of massive or parallel laminated to ripple cross
206 laminated siltstone to fine grained parallel laminated or cross-stratified sandstone (Figs. 6A,
207 6D and 6G). Facies Fm, Fl, Fr, Sl and Sp (Table 1) are represented (Fig. 5A-E). Bed sets
208 commonly show an erosive base with an overall fining upward trend and also record bedform
209 evolution from massive through parallel laminated to ripple laminated facies. These siltstones
210 and fine-grained sandstones are interpreted to record deposition within crevasse splays and
211 crevasse channels, with parallel lamination to ripple lamination within a bed indicating flow
212 deceleration resulting from flow expansion. Sandstone deposition also occurs in 30 m wide
213 crevasse splay channels. Carbonaceous material and wood fragments are found draping ripples
214 and along laminations. These fine-grained overbank deposits, where interbedded with the
215 mudstone, carbonaceous mudstone and thin coal layers, indicate distal floodplain
216 environments (Collinson, 1996).

217 *3.1.3. Floodplain/floodplain pond facies association*

218 This facies association is composed of massive and laminated mudstones (facies C and
219 Cl), coal (facies D), massive, laminated and ripple cross-stratified siltstones (facies Fm, Fl and
220 Fr) and tuff (facies T; Table 1). They occur generally as laterally continuous sheets formed
221 following the decrease in bedform size from ripple scale cross-lamination to the floodplain
222 mudstone and/or coal facies (Figs. 6B, 6E and 6G). These deposits occur in low energy
223 settings on the floodplain.

224

225 3.2. *Depositional environments*

226 3.2.1 *Coal-bearing Permian strata*

227 All three identified facies associations are present within the coal-bearing Permian
228 succession. We did not identify any significant differences between outcrops from the five
229 Permian and Upper Carboniferous suites, although the latter was only studied at one outcrop.
230 The sedimentology of the coal-bearing Permian sections suggests environments of fluvial
231 channels, with extensive overbank areas. Mires within these overbank areas allowed peat
232 deposition. Fining upward packages (localities S-21 (Fig. 6B) and S-22), are interpreted to
233 represent channel avulsion, although they could also result from lateral channel migration.
234 The occurrence of coal facies directly overlain by fluvial sandstones is considered unusual by
235 McCabe (1984) and suggests extreme, far reaching avulsion. Such large-scale avulsion may be
236 a characteristic of anastomosing systems (Makaske, 2001). Fielding (1984) noted that
237 compaction of peat deposits in the Carboniferous Northumberland Basin could produce
238 “basins” tens of kilometres wide, with sharp contacts with overlying sandstones. The
239 association of overbank environments and coal deposition indicates stagnant, long-lived, low
240 relief flood plains. These suggest the overall system had a meandering planform.

241 3.2.2. *End-Permian/Triassic strata*

242 All three facies associations are also present within the end-Permian/Triassic
243 succession, but significant coal seams are not present; coal is reduced to discontinuous
244 millimetre-scale laminae. The abrupt sedimentary contact between the Permian coal measures
245 and overlying sandstones and conglomerates is interpreted to represent the rapid change from
246 peat formation in a floodplain swamp to deposition from large in-channel barforms following
247 avulsion with an increase to a high energy bedload, fluvial system (Fig. 7b). The initial sand
248 grade deposition occurs in foresets with a preserved set thickness of at least 20 m indicating
249 lateral barform migration. The current geometry of the beds, which appear over steepened

250 (Fig. 5G), and ‘doming’ above the underlying coal, are due to compaction effects (Fielding,
251 1984). There appears to be no change in foreset steepness upwards, indicating no preservation
252 of topsets, therefore suggesting bedforms were at least 20 m in height, with an even deeper
253 channel. A cross section through a similar sized bar form, composed of sand grade material at
254 locality S-14 (Fig. 6C), indicates the main fluvial flow direction was to the northeast. The
255 width of the channels forming these bars is harder to quantify. The lateral extent of the sand
256 grade barform is at least 150 m and so the channel width may have been in the order of several
257 kilometres wide. The enormous lateral scale of the barforms and the fluvial systems in which
258 they formed suggests a major increase in the rivers’ capacity at this time, despite a possible
259 decrease in channel depth in comparison to the underlying coal-bearing Permian sediments.
260 The dominant coarse grain size of these systems indicates deposition from high velocity flows
261 over the floodplain and a likely braided planform. The depositional setting for the finer
262 sandstones and gravel sediments is within a mixed load system, and within an overbank
263 setting derived from crevasse splays, crevasse channels and long lived floodplain lake
264 environments in the fluvial floodplain (Fig. 7c), and indicates these systems were meandering.

265 *3.2.3. Jurassic and Cretaceous strata*

266 All three facies associations are also present within the Jurassic succession. The
267 observed sedimentology in the exposed Jurassic sections in the Kuznetsk Basin indicate
268 deposition from a mainly mixed to bedload-dominated fluvial system. This system resulted in
269 the deposition of laterally extensive sheets of conglomerates with channels containing sands,
270 indicating periods of lower flow velocities, deposited in shallow water depths of several
271 metres. Channel abandonment is recorded by the overall fining up of sediment from
272 conglomerates, through sandstone and siltstones to mudstone and eventually the accumulation
273 of organic matter now preserved as minor coal (Fig. 6F). Overbank environments can also be
274 seen within the Jurassic section with crevasse splay deposited sands interbedded with

275 mudstones and coals (Fig. 6G). The Jurassic section contains the largest clasts (60 cm) and
276 also the thickest conglomeratic succession (several 10s of metres) of the entire basin
277 stratigraphy. This implies that during deposition of the Jurassic strata, river gradients and
278 stream power were greater than during earlier deposition, in turn implying closer and/or
279 greater source area relief. These coarse clastic, higher energy systems are likely to have had a
280 braided planform (Fig. 7d). The localised finer grained parts of the stratigraphic interval
281 indicate a reduction in fluvial energy, either lateral to the main trunk system or by channel
282 abandonment.

283 It is not possible to be certain of the relevant facies association(s) for the Cretaceous
284 strata because of the limited nature of the outcrop in the southwest corner of the basin (Fig. 2).
285 Mudstones are laminated, brick red in colour and have occasional silty laminations and are
286 occasionally interbedded with parallel to ripple cross laminated very fine-grained sandstone.
287 Vertical burrows, 0.5-1 cm in diameter, are formed in the sandstone and infilled with
288 mudstone.

289

290 *3.3. Palaeocurrent analysis*

291 *3.3.1. Coal-bearing Permian*

292 Palaeoflow directions derived from the Permian fluvial channel belt deposits show that
293 the dominant sediment transport direction was to the northwest, northeast and east, depending
294 on the position within the Kuznetsk Basin (Fig. 8). Rivers flowed towards the interior of the
295 West Siberian Basin. This implies a possible source area from the terranes of the Gornyy Altai
296 to the south and maybe some sediment derived from the Salair Range to the west. Within the
297 overbank facies of Permian age, ripples indicate dominant flow directions to the northeast and
298 northwest (Fig. 8). Unidirectional ripples also clearly show palaeoflow to the east (locality S-
299 7).

300 3.3.2. *End-Permian/Triassic*

301 The end-Permian/Triassic rocks show a palaeoflow to the north and northeast, with a
302 likely sediment source area in the Gorny Altai, as seen for the coal-bearing Permian (Fig. 8).
303 Clast compositions of tuff, basalt, chert and limestone are also consistent with derivation from
304 the Gorny Altai to the south. Palaeoflow directions from the large-scale foresets in the
305 conglomerates at locality S-16 and the sand grade material at locality S-17 record cross
306 channel migration of bar margin slipfaces (Best *et al.*, 2003), resulting in the lateral migration
307 of these large bar forms, to the southeast or east, allowing an assumption that the main fluvial
308 system trended roughly NE-SW. The end-Permian/Triassic strata contain ripples with a
309 probable dominant flow to the southwest.

310 3.3.3. *Jurassic*

311 Jurassic palaeocurrent indicators in fluvial channel belt deposits record flow
312 dominantly towards the northeast or northwest, again indicating a source area to the south of
313 this region (Fig. 8). This is confirmed by the clast lithologies, which appear to be derived
314 from the Gorny Altai, to the south of the Kuznetsk Basin. Within the finer-grained Jurassic
315 strata, a ripple crest orientation of northwest-southeast and a slight asymmetry, indicates a
316 dominant flow direction of these low energy currents to the northeast (Fig. 8). We have no
317 robust dataset for the Cretaceous rocks.

318 Overall, there are no significant compositional changes in clast-type found in the
319 Permian, Triassic or Jurassic strata. The clast compositions suggest that the volcanics, low
320 grade metasediments and melanges of the Gorny Altai sourced the observed sediments. This
321 is in contrast with the modern Tom' River through the Kuznetsk Basin, where many granitic
322 clasts occur, derived from the basement of the Kuznetsk Alatau to the east of the basin.

323

324 **4. Deformation**

325 This section considers the structures, boundaries and sedimentology of the Kuznetsk
326 Basin strata in terms of what they reveal about the timing and nature of regional deformation.
327 The >5 km thick Upper Carboniferous-Permian succession of the basin interior appears to
328 have been deposited without major internal unconformities or syn-sedimentary faulting. The
329 deposits lie between the fold and thrust belts at the basin margins (Fig. 2). Permian strata at
330 the western basin margin are folded in to a sub-vertical orientation. Although the movement
331 history on the marginal thrusts is not well-constrained, it is feasible that they operated during
332 the Late Carboniferous and Permian to create accommodation space in their forelands – i.e.
333 the Kuznetsk Basin. This timing is the late stage of assembly of the Altaid orogenic collage,
334 including the collision of the Tarim Block along its southern margin. There is no evidence of
335 Early Permian rifting, reported for parts of northwest China (Wartes et al., 2002).

336 There is no indication of any local tectonism associated with the end-Permian basalts,
337 such as regional uplift or rifting. As they are only a few metres thick, it is likely that they
338 represent the extreme edge of the Siberian flood basalt magmatism, which reaches a thickness
339 of ~3 km in the northwest of the Siberian Craton near Noril'sk (~1700 km north of the
340 Kuznetsk Basin), but only ~50 m at the southeast of the outcrop limit on the craton (~700 km
341 from the Kuznetsk Basin basalts; Lightfoot et al., 1993; Reichow et al., 2009). Therefore there
342 is no local evidence for a tectonic event (tilting, faulting, abrupt provenance shifts) at the
343 Permian-Triassic boundary changing the depositional regime in the Kuznetsk Basin, but an
344 environmental crisis caused by the Siberian flood basalts is plausible.

345 The Jurassic succession lies unconformably over the end-Permian and Triassic(?)
346 rocks. This implies folding and erosion of the basin interior before the deposition of the
347 Jurassic strata. The amount of erosion was in places enough to remove most of the Permian
348 succession, implying several kilometres of erosion (Fig. 2). Nowhere is any Late Triassic
349 mapped, but it is not clear if this reflects later erosion, original non-deposition, or the

350 difficulties in dating a non-marine clastic succession. The base of the Jurassic may be either a
351 disconformity, without a discordance in bedding or an angular unconformity with a
352 discordance of a few degrees (Fig. 9). The earliest Jurassic strata are conglomeratic in the
353 localities studied, indicating that there was considerable relief in the sediment source areas
354 and high stream power at this time. Jurassic strata are themselves folded (Fig. 2), so that there
355 is clearly also deformation that postdates this period.

356 The timing of the deformation recorded below the base of the Jurassic is constrained to
357 post-date at least part of the Middle Triassic, which is the age assigned to the youngest
358 Triassic preserved, and to pre-date at least part of the Early Jurassic, which is the age of the
359 oldest Jurassic strata. More precise constraints are not available from the field relations or the
360 current knowledge of the age of the affected stratigraphy. The age of the deformation that
361 post-dated the Jurassic strata is less well constrained. It is plausibly around the Jurassic-
362 Cretaceous boundary, for two reasons. First, the sparse Cretaceous outcrops are in a
363 completely different part of the Kuznetsk Basin to the Jurassic, in the southwest (Fig. 2). This
364 may imply a reconfiguration of the basin at or before this time. Second, to the northeast of the
365 Kuznetsk Basin, on the southern side of the West Siberian Basin, there is a minor angular
366 unconformity mapped between Jurassic and Early Cretaceous strata. As Cretaceous strata are
367 themselves tilted at up to 50° in the southwest of the Kuznetsk Basin, there has clearly been
368 deformation after this time too, although this is not discernible as a discrete phase in the
369 structure of the Triassic and Jurassic outliers. This later deformation event may have taken
370 place in the Late Cretaceous, as much of Central Asia was reduced to a peneplain at the end of
371 this period (Allen et al., 2001). It could be Cenozoic, although the Kuznetsk Basin is not
372 seismically active. There is geomorphologic evidence for subtle young or active deformation,
373 in the form of systematic lateral shifts of drainage (Allen and Davies, 2007).

374 End-Permian and Triassic(?) and Jurassic strata within the basin interior are preserved
375 in three major outliers and a small number of adjacent outliers. The central and southern
376 outliers are very open synclines, with half wavelengths in the order of 10s of kilometres (Fig.
377 2). They are associated with smaller, parasitic, folds on wavelengths of the order of
378 kilometres to hundreds of metres. Dips associated with Jurassic strata on these local
379 structures reach $\sim 40^\circ$.

380 The largest Mesozoic outlier lies in the centre of the Kuznetsk Basin and is aligned
381 roughly northwest-southeast, i.e. roughly parallel to the main axis of the basin, and to the
382 thrusts of the Salair Range. The second largest outlier is in the south, and is aligned roughly
383 northeast-southwest, sub-parallel to the structural trends in the Permian and older rocks to its
384 south, at the basin margin. The third outlier was not studied during our fieldwork, and lies at
385 the intersection of the Salair and Tom' Kolyvan ranges to the north of the study area, trending
386 roughly east-west. Unlike the other two, it is not synformal, but all strata appear to be tilted to
387 the north, beginning with strata mapped as Upper Triassic (an age not found further south),
388 which lie unconformably over folded older rocks.

389 The "bullseye" appearance of the Mesozoic synclines in map view resembles folds
390 produced by Type 1-2 refolding, i.e. the basins of dome-and-basin refolds (Ramsay and
391 Huber, 1987), but there is no positive evidence that this has taken place, in the form of
392 overprinting of structures. It is also plausible that the present structural patterns result from
393 synchronous or near-synchronous compression from more than one basin margin, in the
394 manner of the active tectonics of the South Caspian Basin (Jackson et al., 2002).

395

396 **5. Discussion**

397

398 *5.1. End-Permian environments*

399 Deposition in the Kuznetsk Basin spanned the Permian-Triassic transition and
400 included basalts of the Siberian Traps large igneous province. Therefore the basin fill provides
401 a record of terrestrial environmental changes during the greatest global mass extinction event,
402 in a region affected by the magmatism commonly interpreted as the cause of the
403 environmental and biotic crisis (Wignall, 2001). The top of the Permian coal measures is
404 marked by an abrupt transition to coal-barren, sand dominated large scale foresets of a
405 laterally accreting barform, before being overlain by conglomeratic beds interpreted as the
406 deposits of a high energy bedload fluvial system. Features include downlap geometries on to
407 the underlying coals, but are likely sedimentary/compaction in origin, and not an angular
408 unconformity or other indication of tectonic activity.

409 The disappearance of coals some 50 m below the lowest basalt (dated at 250.3 ± 0.7
410 Ma by Reichow et al., 2009) indicates that the environmental crisis in the Kuznetsk Basin
411 occurred slightly before the first flood basalt magmatism affected this area. Given that many
412 precise age determinations for the Siberian Traps are slightly older than the Kuznetsk basalts
413 (Reichow et al., 2009) it is still feasible that the Siberian Trap magmatism caused the global
414 environmental crisis and mass extinction. This is in keeping with the type Permo-Triassic
415 boundary section at Meishan, China, where the extinction peaked at the top of Bed 24 (Jin et
416 al., 2000), below the biostratigraphical Permo-Triassic boundary at the base of Bed 27c
417 (defined by the first appearance of the conodont *Hindeodus parvus*; Nicoll et al., 2002).

418 The nature of the crisis is similar to other terrestrial regions at the time, including the
419 Urals foreland (Newell et al., 1999; Benton, 2008) and the Bowen Basin, Australia
420 (Michaelsen, 2002): catastrophic loss of vegetation and a presumed increase in aridity
421 (reflected in the disappearance of coal measures), followed by an increase in sediment grade
422 (presumably erosion was enhanced by the widespread loss of vegetation). The energy of the
423 depositional systems fluctuated above this environmental crisis, but the extensive vegetation

424 cover did not return until the Jurassic, based on the record of coal seams. The Kuznetsk Basin
425 succession is therefore consistent with the global Early-Middle Triassic coal gap (Retallack et
426 al., 1996), given that there are no coal seams in the end-Permian-Triassic strata, which are
427 supposed to extend up to the Middle Triassic (Mogutcheva and Krugovykh, 2009). It is more
428 extreme than other areas where Middle Triassic coal is recorded. As no Upper Triassic strata
429 are reported from the Kuznetsk Basin it is not known whether coal-forming conditions
430 recovered in the Late Triassic.

431

432 *5.2. Implications for Central Asian tectonics*

433 The Permian-Triassic succession in the Kuznetsk Basin shows no evidence for the
434 extensional faulting that created the West Siberian Basin. It may be that the southern margin
435 of the Kuznetsk Basin was beyond the rifting limit. The Triassic is relatively thin (300-460 m)
436 in the Kuznetsk Basin, and suggests lower subsidence rates than during the Permian. This is
437 consistent with a regional switch-off of compressional tectonics during the end-Permian
438 rifting of the West Siberian Basin and the eruption of the Siberian Traps (Allen et al., 2006).

439 Compressional deformation affected all of the Permian-Triassic sediments within the
440 Kuznetsk Basin, indicated by folding of the end-Permian/Triassic deposits and the angular
441 unconformity at the base of the Jurassic succession. The Late Triassic-Early Jurassic was a
442 time of regional deformation across much of Central Asia, associated with the Palaeo-Tethyan
443 collision of Gondwana-derived microcontinents with the southern margin of Asia. This has
444 left a widespread record of angular unconformities, fold-and-thrust belts and exhumation
445 (Hendrix et al., 1992; Allen and Vincent, 1997; Vincent and Allen, 2001; De Grave et al.,
446 2007). An unconformity is also present at the base of the Jurassic section in the Mariinsk-
447 Krasnoyarsk region to the east of the Kuznetsk Basin (Le Heron et al., 2008).

448 It is likely that the deformation below the basal Jurassic unconformity in the Kuznetsk
449 Basin represents part of this regional tectonics, and the overlying Jurassic strata relate to
450 rejuvenation of marginal thrust belts, and a resultant flexural loading. The Jurassic strata
451 initially dominantly contain conglomeratic beds, but no further unconformities or laterally
452 extensive sedimentary pulses. The succession generally fines upwards, with the reappearance
453 of coal measures, possibly at the end of the Early Jurassic or in the Middle Jurassic. This
454 pattern differs from other Central Asian basins such as Junggar, where there are several
455 unconformities and sedimentary pulses within the Jurassic (Hendrix et al., 1992; Vincent and
456 Allen, 2001; Greene et al., 2005), related to the further Tethyan orogenies at the evolving
457 Eurasian continental margin.

458 Folding of the Jurassic strata (Fig. 2) have taken place in the Late Jurassic or Early
459 Cretaceous, because Upper Jurassic strata are not known from the basin. De Grave et al.
460 (2007) produced fission track data for extensive uplift in Central Asia in the time range 140-
461 100 Ma, i.e. Late Jurassic to mid Cretaceous.

462 Thin Cretaceous deposits may represent a short-lived record of transgression during
463 some part of this period. The 50° bedding dip in one outcrop in the study area indicates
464 tectonism post-dating deposition, but there are no good time constraints.

465

466 *5.3. Implications for the West Siberian Basin*

467 The Kuznetsk Basin is ~300 km from the southern edge of the West Siberian Basin, so
468 that its evolution can shed light on this major hydrocarbon province, in particular in the
469 identification of sediment transport pathways. The sediments during and immediately after the
470 end-Permian environmental crisis are composed of coarse clastic conglomerates deposited
471 from high stream power bedload systems. These systems had higher stream power when
472 compared to the rest of the Permian, and sediment is likely to have been bypassed into the

473 West Siberian Basin interior, at the very time rifting was underway. The rest of the end-
474 Permian and Triassic(?) is finer-grained fluvial and overbank deposits from lower energy
475 systems, with less chance of these later sediments being exported to the West Siberian Basin
476 interior.

477 The basal Jurassic unconformity represents sediment erosion (of the Triassic and
478 Permian strata) and its possible transfer into the West Siberian Basin. The deformation
479 associated with this feature presumably led to the uplift of the hinterland (Gorny Altai) and a
480 renewed pulse of coarse clastic sediment input into the Kuznetsk Basin by shallow, high
481 stream power, fluvial systems. This implies a likely pulse of Early Jurassic siliciclastics into
482 the West Siberian Basin from the south. These sediments are unlikely to make good
483 hydrocarbon reservoir sandstones: Altaid lithologies are commonly slates, other low grade
484 metamorphics and basic volcanics.

485 The fining-up nature of the Jurassic succession implies that it would have been a
486 decreasing source of sediment for the West Siberian Basin over time. The thin, fine-grained
487 Cretaceous succession in the Kuznetsk Basin suggests no uplift in the surrounding hinterland,
488 in contrast to the southeast flank of the West Siberian Basin (Le Heron et al., 2008). This
489 tallies with the ~800-1000 m thick main Neocomian reservoir unit of the West Siberian Basin
490 prograding in to the basin interior from the east and west, with little sediment input from the
491 south (Peterson and Clarke, 1991).

492

493 **6. Conclusions**

494 Permian and Mesozoic sediments within the Kuznetsk Basin are non-marine
495 siliciclastics deposited in fluvial environments. They are grouped in three facies associations:
496 i) fluvial channel belt ii) overbank and iii) floodplain/floodplain pond. The latter association
497 includes extensive coal deposits, particularly in the 5 km thick Permian succession. Permian

498 sedimentation is interpreted as a response to thrust-sheet loading from the basin margins. An
499 environmental crisis at the end of the Permian led to the loss of the vegetation that produced
500 the coal seams, and is interpreted as part of the global biotic catastrophe near the Permian-
501 Triassic boundary. Sediments immediately above the coals are thicker and coarser
502 siliciclastics, probably produced when source areas were rapidly eroded once they had lost
503 their vegetation cover. Basalt flows within the basin are part of the Siberian Traps, and occur
504 just above the environmental change. A precise Ar-Ar age from the lower flow of 250.3 ± 0.7
505 Ma (Reichow et al., 2009) indicates that the adjacent sediments are Late Permian, and that the
506 Permian-Triassic boundary lies some way above this flow, and therefore slightly later than the
507 environmental change.

508 A gentle angular unconformity at the base of the Jurassic succession plausibly
509 correlates with Late Triassic-Early Jurassic deformation recorded from elsewhere in Central
510 Asia, related to Palaeo-Tethyan closure and continental collision at the southern Eurasian
511 margin. Overlying Jurassic strata are themselves folded, but the timing and nature of this
512 event is more obscure. The Cretaceous is represented by thin, poorly-exposed strata, that are
513 difficult to place in a regional context. There is a marked contrast between the Cretaceous
514 evolution of the Kuznetsk Basin and the Mariinsk-Krasnoyarsk region to the east and the West
515 Siberian Basin to the north (Le Heron et al., 2008). Both of the latter areas are marked by a
516 resurgence of sedimentation in the Early Cretaceous. Some deformation postdates the
517 Cretaceous deposits in the Kuznetsk Basin: they are at least locally tilted at 50° , while the
518 modern basin has lateral drainage shifts indicative of subtle, long wavelength deformation at
519 the edge of the India-Asia collision (Allen and Davies, 2007).

520

521 **Acknowledgements**

522

523 This study was carried out when two of the authors (CD and MA) were at CASP,
524 Department of Earth Sciences, University of Cambridge, and CASP are thanked for
525 permission to publish. We also thank the industrial sponsors of the West Siberian Basin
526 Project. The Institute of Geology and Mineralogy, Russian Academy of Sciences,
527 Novosibirsk, provided support. We also thank Nikolai Semakov and Lena Soloboeva for their
528 assistance during the field campaign. Two anonymous referees provided helpful reviews.
529
530

531 **References**

532

533 Al'mukhamedov, A.I., Medvedev, A.Y., Kirda, N.P., Baturina, T.P., 1998. The Triassic
534 volcanogenic complex of western Siberia. *Doklady Earth Sciences* 362, 931-935.

535 Allen, M.B., Alsop, G.I., Zhemchuzhnikov, V.G., 2001. Dome and basin refolding and
536 transpressive inversion along the Karatau Fault System, southern Kazakstan. *Journal*
537 *of the Geological Society, London* 158, 83-95.

538 Allen, M.B., Anderson, L., Searle, R.C., Buslov, M.M., 2006. Oblique rift geometry of the
539 West Siberian Basin: tectonic setting for the Siberian flood basalts. *Journal of the*
540 *Geological Society, London* 163, 901-904.

541 Allen, M.B., Davies, C.E., 2007. Unstable Asia: active deformation of Siberia revealed by
542 drainage shifts. *Basin Research* 19, 379-392.

543 Allen, M.B., Vincent, S.J., 1997. Fault reactivation in the Junggar region, northwest China:
544 the role of basement structures during Mesozoic-Cenozoic compression. *Journal of the*
545 *Geological Society, London* 154, 151-155.

546 Ashley, G.M., 1990. Classification of large-scale subaqueous bedforms: A new look at an old
547 problem. *Journal of Sedimentary Petrology* 60, 160-172.

548 Benton, M.J., 2008. The end-Permian mass extinction events on land in Russia. *Proceedings*
549 *of the Geologists Association* 119, 119-136.

550 Best, J.L., Ashworth, P.J., Bristow, C.S., Roden, J., 2003. Three-dimensional sedimentary
551 architecture of a large, mid-channel sand braid bar, Jamuna River, Bangladesh. *Journal*
552 *of Sedimentary Research* 73, 516-530.

553 Buslov M.M., Safonova I.Yu., Fedoseev G.S., Reichow M., Travin A.V., Babin G.A., 2007.
554 Plume-related basalts of the Kuznetsk Basin. In: R. Seltmann, A. Borisenko, G.
555 Fedoseev (Editors), *Magmatism and Metallogeny of the Altai and Adjacent Large*

- 556 Igneous Provinces with an Introductory Essay on the Altaids, IAGOD Guidebook
557 Series 16, CERCAMS/NHM, London, pp. 121-135.
- 558 Buslov M.M., Watanabe T., Fujiwara Y., Iwata K., Smirnova L.V., Safonova I. Yu., Semakov
559 N.N., Kiryanova A.P., 2004. Late Paleozoic faults of the Altai region, Central Asia:
560 tectonic pattern and model of formation. *Journal of Asian Earth Sciences* 23, 655-671.
- 561 Collinson, J.D., 1996. Alluvial sediments. In: H.G. Reading (Editor), *Sedimentary*
562 *environments: Processes, Facies and Stratigraphy*. Blackwell Science, Oxford, pp. 37-
563 82.
- 564 Cook, H.E., Zhemchuzhnikov, V.G., Buvtyshkin, V.M., Golub, L.Y., Gatovsky, Y.A., Zorin,
565 A.Y., 1995. Devonian and Carboniferous passive-margin carbonate platform of
566 southern Kazakhstan: summary of depositional and stratigraphic models to assist in the
567 exploration and production of coeval giant carbonate platform oil and gas fields in the
568 north Caspian Basin, western Kazakhstan. *Pangea: Global Environments and*
569 *Resources*. Canadian Society of Petroleum Geologists Memoir, pp. 363-381.
- 570 De Grave, J., Buslov, M.M., Van den Haute, P., 2007. Distant effects of India-Asia
571 convergence and Mesozoic intracontinental deformation in Central Asia: constraints
572 from apatite fission-track thermochronology. *Journal of Asian Earth Sciences* 29, 188-
573 204.
- 574 Esaulova, N.K., 1997. Correlation of Upper Permian deposits in the Volga-Urals region and
575 Kuznetsk basin. *Stratigraphy and Geological Correlation* 5, 468-477.
- 576 Fielding, C.R., 1984. A coal depositional model for the Durham Coal Measures of NE
577 England. *Journal of the Geological Society*, London 141, 919-939.
- 578 Greene, T.J., Carroll, A.R., Wartes, M., Graham, S.A., Wooden, J.L., 2005. Integrated
579 provenance analysis of a complex orogenic terrane: Mesozoic uplift of the Bogda Shan

- 580 and inception of the Turpan-Hami Basin, NW China. *Journal of Sedimentary Research*
581 75, 251-267.
- 582 Gutak, J.M., Tolokonnikova, Z.A., Ruban, D.A., 2008. Bryozoan diversity in Southern Siberia
583 at the Devonian-Carboniferous transition: New data confirm a resistivity to two mass
584 extinctions. *Palaeogeography, Palaeoclimatology, Palaeoecology* 264, 93-99.
- 585 Hendrix, M.S., Graham, S.A., Carroll, A.R., Sobel, A.R., McKnight, C.L.S., B. S., Wang, Z.,
586 1992. Sedimentary record and climatic implications of recurrent deformation in the
587 Tian Shan: Evidence from Mesozoic strata of the North Tarim, South Junggar, and
588 Turpan basins, northwest China. *Bulletin of the Geological Society of America* 104,
589 53-79.
- 590 Jackson, J., Priestley, K., Allen, M., Berberian, M., 2002. Active tectonics of the South
591 Caspian Basin. *Geophysical Journal International* 148, 214-245.
- 592 Jin, Y.G., Wang, Y., Wang, W., Shang, Q.H., Cao, C.Q., Erwin, D.H., 2000. Pattern of marine
593 mass extinction near the Permian-Triassic boundary in South China. *Science* 289, 432-
594 436.
- 595 Kurtigeshev, V.S., Rodchenko, S.A., Mitrokhin, D.V., Tumanova, L.N., Tokarev, V.N.,
596 Babin, G.A., 2008. 1:200,000 State Geological Map of the Russian Federation Sheet
597 N-45-X (Central Kuzbass). Kartfabrika VSEGEI, Saint Petersburg.
- 598 Lavrenov, P.F., Snezhko, B.A., Schigrev, A.F., Shelemeteva, N.V., Filippova, N.E., 2008.
599 1:200,000 State Geological Map of the Russian Federation Sheet N-45-XV (Leninsk-
600 Kuznetsky). Kartfabrika VSEGEI, Saint Petersburg.
- 601 Le Heron, D.P., Buslov, M.M., Davies, C., Richards, K., Safonova, I., 2008. Evolution of
602 Mesozoic fluvial systems along the SE flank of the West Siberian Basin, Russia.
603 *Sedimentary Geology* 208, 45-60.

- 604 Leclair, S.F., Bridge, J.S., Wang, F.Q., 1996. Preservation of cross-strata due to migration of
605 subaqueous dunes over aggrading and non-aggrading beds: Comparison of
606 experimental data with theory, Symposium on From Sandstone to Chaos at the Annual
607 Meeting of the Geological Society of America, Northeastern Section. Geological
608 Assoc Canada, Buffalo, New York, pp. 55-66.
- 609 Lightfoot, P.C., Hawkesworth, C.J., Hergt, J., Naldrett, A.J., Gorbachov, N.S., Fedorenko,
610 V.A., Doherty, W. 1993. Remobilization of the continental lithosphere by a mantle
611 plume - major element, trace element and Sr-isotope, Nd-isotope and Pb-isotope
612 evidence from picritic and tholeiitic lavas of the Norilsk district, Siberian Trap,
613 Russia. Contributions to Mineralogy and Petrology 114, 171-188.
- 614 Makaske, B., 2001. Anastomosing rivers: a review of their classification, origin and
615 sedimentary products. Earth Science Reviews 53, 149-196.
- 616 McCabe, P.J., 1984. Depositional environments of coal and coal-bearing strata. In: R.A.
617 Rahmani and R.M. Flores (Editors), Sedimentology of coal and coal-bearing
618 sequences. Special Publication of the International Association of Sedimentologists,
619 pp. 13-42.
- 620 Michaelsen, P., 2002. Mass extinction of peat-forming plants and the effect on fluvial styles
621 across the Permian-Triassic boundary, northern Bowen Basin, Australia.
622 Palaeogeography, Palaeoclimatology, Palaeoecology 179, 173-188.
- 623 Mogutcheva, N.K., 2009. Problems of phytostратigraphy and the correlation of the Lower
624 Jurassic continental sediments in West Siberia and Kuznetsk and Kansk-Achinsk
625 basins. Stratigraphy and Geological Correlation 17, 283-290
- 626 Mogutcheva, N.K., Krugovykh, V.V., 2009. New data on the stratigraphic chart for Triassic
627 deposits in the Tunguska syncline and Kuznetsk basin. Stratigraphy and Geological
628 Correlation 17, 510-518.

- 629 Newell, A.J., Tverdokhlebov, V.P., Benton, M.J., 1999. Interplay of tectonics and climate on a
630 transverse fluvial system, Upper Permian, Southern Uralian Foreland Basin, Russia.
631 *Sedimentary Geology* 127, 11-29.
- 632 Nicoll, R.S., Metcalfe, I., Wang, C.Y., 2002. New species of the conodont Genus *Hindeodus*
633 and the conodont biostratigraphy of the Permian-Triassic boundary interval. *Journal of*
634 *Asian Earth Sciences* 20, 609-631.
- 635 Peterson, J.A., Clarke, J.W., 1991. Geology and hydrocarbon habitat of the West Siberian
636 Basin. AAPG Studies in Geology No. 32. AAPG, 96 pp.
- 637 Ramsay, J.G., Huber, M.I., 1987. *The Techniques of Modern Structural Geology Volume 2,*
638 *Folds and Fractures.* Academic Press, London, 309-700 pp.
- 639 Reichow, M.K., Pringle, M.S., Al'Mukhamedov, A.I., Allen, M.B., Andreichev, V.L., Buslov,
640 M.M., Davies, C.E., Fedoseev, G.S., Fitton, J.G., Inger, S., Medvedev, A.Ya.,
641 Mitchell, C., Puchkov, V.N., Safonova, I.Yu., Scott, R.A., Saunders, A.D., 2009. The
642 timing and extent of the eruption of the Siberian Traps large igneous province:
643 Implications for the end-Permian environmental crisis. *Earth and Planetary Science*
644 *Letters* 277, 9-20.
- 645 Renne, P.R., Zichao, Z., Richards, M.A., Black, M.T., Basu, A.R., 1995. Synchrony and
646 causal relations between Permian–Triassic boundary crises and Siberian flood
647 volcanism. *Science* 269, 1413–1416.
- 648 Retallack, G.J., Veevers, J.J., Morante, R., 1996. Global coal gap between Permian-Triassic
649 extinction and Middle Triassic recovery of peat-forming plants. *Geological Society of*
650 *America Bulletin* 108, 195-207.
- 651 Şengör, A.M.C., Natal'in, B.A., 1996. Paleotectonics of Asia: fragments of a synthesis. In: A.
652 Yin and M. Harrison (Editors), *The Tectonic Evolution of Asia.* Cambridge University
653 Press, Cambridge, pp. 486-640.

- 654 Usov, M.A., 1937. The Trap Formation of the Kuznetsk Basin. *Izvestia Akademia Nauk*
655 *SSSR, Geology Series 4*, 743-763.
- 656 Vincent, S.J., Allen, M.B., 2001. Sedimentary record of Mesozoic intracontinental
657 deformation in the eastern Junggar Basin, northwest China: Response to orogeny at the
658 Asian margin, *Memoirs of the Geological Society of America* 194, pp. 341-360.
- 659 Vyssotski, A.V., Vyssotski, V.N., Nezhdanov, A.A., 2006. Evolution of the West Siberian
660 Basin. *Marine and Petroleum Geology* 23, 93-126.
- 661 Wignall, P.B., 2001. Large igneous provinces and mass extinctions. *Earth-Science Reviews*
662 53, 1-33.
- 663 Yavorskiy, V.I., Butov, P.I., 1927. Kuznetsk coal-bearing basin. Geolkom Publications,
664 Leningrad, 244 pp.
- 665 Zonenshain, L.P. Mezhelovsky, N.V., Natapov, L.M., 1988. 1:2,000,000 Geodynamic map of
666 the USSR and adjacent seas. Ministry of Geology of the USSR.
- 667

668 **Figure captions**

669 **Fig. 1.** a) Location map of the Kuznetsk Basin, showing its proximity to the West Siberian
670 Basin to the north. Shaded digital topography from the GTOPO30 dataset. b) Structural
671 framework of the Kuznetsk Basin, showing its proximity to marginal fold and thrust belts, and
672 location south of the main West Siberian Basin. Fault locations adapted from Zonenshain et
673 al. (1988) and Allen et al. (2006).

674 **Fig. 2.** Geology map of the Kuznetsk Basin (Buslov et al., 2007; Kurtigeshev et al., 2008;
675 Lavrenov et al., 2008).

676 **Fig. 3.** Stratigraphic table for the Kuznetsk Basin. From Buslov et al. (2007) and earlier
677 sources, e.g. Yavorskiy and Butov (1927).

678 **Fig. 4.** Summary log for the Kuznetsk Basin. From Buslov et al. (2007) and our field
679 observations.

680 **Fig. 5.** Examples of sedimentary facies from the Permian, end-Permian/Triassic and Jurassic
681 of the Kuznetsk Basin. **(A)** The base of the outcrop is dominated by dark grey massive (*C*) to
682 laminated mudstones (*Cl*) grading to carbonaceous rich laminated mudstones (*Cl*) with
683 millimetre thick coal beds above (*D*), before further grey mudstones are deposited on top.
684 Notebook for scale. Locality S-7; Jurassic. **(B)** Interbedded mudstone and carbonaceous
685 mudstone (*Cl*), siltstone (*F*, *Fl*) and very fine grained massive and parallel laminated
686 sandstones (*Sm*, *Sl*) are interpreted as alluvial overbank deposits. The bedding dip is structural
687 in origin. Locality S-7; Jurassic. **(C)** Laterally continuous massive mudstone (*C*) layers
688 commonly occur within the thick coal (*D*) units. The truck (circled) is ~4 m high. Locality S-
689 16; Permian. **(D)** Parallel laminated siltstone (*Fl*) and very fine grained sandstones (*Sl*) occur
690 with black organic fragments highlighting the lamination surfaces. Pencil top is ~2.5 cm.
691 Locality S-7; Permian. **(E)** Ripple foresets within the siltstones (*Fr*) and very fine grained
692 sandstones (*Sr*), with foresets highlighted by organic fragments, some ripples are possibly

693 climbing. Pencil is ~9 cm. Locality S-7; Permian. **(F)** Planar and trough cross-stratified
 694 sandstones (*Sp*, *St*) contain varying amounts of rounded to well rounded pebbles, 0.2-6 cm in
 695 length, aligned along foresets and along scoured channel bases. Set thickness is 0.5-1m.
 696 Locality S-21; Permian. **(G)** Apparent downlap of a 30 m thick section of interbedded
 697 sandstones (*Sl*, *Sr*) and mudstones (*C*, *Cl*) onto the underlying coal unit (*D*). Person (circled)
 698 for scale. This apparent geometry is likely to be due to over-steepening of the overlying beds
 699 during compaction of peat into coal. Locality S-14; Permian. **(H)** Abrupt basal contact of a 20
 700 m thick amalgamated fluvial sand body (*Sm*, *Sp*, *St*) overlying a thick, uniform coal deposit
 701 (*D*). Locality S-21; Permian. **(I)** Clast supported conglomerate (*Gm*), with rounded to
 702 subrounded clasts usually 0.5-10 cm in length, maximum clast size is 30 cm. Hammer is 30
 703 cm. Locality S-6; Jurassic. **(J)** Green coloured laminated mudstone (*Cl*) containing white
 704 layers of tuff (*T*) overlain by a 2 m thick brown weathered basalt layer. Locality S-4; end-
 705 Permian/Triassic. **(K)** 20 m high large scale foresets composed of well rounded clast
 706 conglomerate (*Gp*) deposited with a sharp, non-erosive loaded contact onto the underlying
 707 coal horizon (*D*). The truck (circled) is ~ 4 m high. Locality S-16; Permian and end-
 708 Permian/Triassic.

709 **Fig. 6.** Measured sedimentary logs constructed from seven separate localities where the facies
 710 were identified for the Permian, Triassic and Jurassic in the Kuznetsk region. The logs consist
 711 of a lithological column, a grainsize/sedimentary structures column, arrows which indicate
 712 any measured palaeocurrents and the identified facies for each section. Detailed facies
 713 descriptions are in Table 1. Note the vertical scale varies significantly from log to log.
 714 Localities are shown on Fig. 2.

715 **Fig. 7.** Palaeogeographic illustrations for the interpreted depositional systems of the Kuznetsk
 716 Basin during the Permian to Jurassic. The Permian contained mixed to bedload dominated
 717 fluvial systems, possibly meandering with extensive overbank environments where peat

718 accumulation occurred in low-lying and/or raised mires. The end-Permian/Early Triassic
719 environments underwent a rapid change to bedload dominated, probably braided systems
720 following the climatic crisis resulting in increased runoff due to lack of vegetation. The later
721 end-Permian/Triassic environment indicates a wide fluvial plain containing mixed load fluvial
722 systems, probably meandering, with overbank deposits and lakes. The Jurassic environment
723 contained bedload dominated, possibly braided fluvial systems. The thick conglomeratic
724 succession suggests greater uplift of the Altai/more proximal position of the encroaching
725 thrust sheets than at any other time in the Mesozoic. Coals show the re-colonisation of the
726 floodplain and surrounding areas following the climatic crisis.

727 **Fig. 8.** Palaeocurrent measurements from the Kuznetsk Basin. There is no correction for any
728 later tectonic tilt.

729 **Fig. 9.** Field evidence for deformation within the Kuznetsk Basin from locality S-24: angular
730 unconformity at the base of the Jurassic succession. Arrows highlight a fracture set within the
731 Permian strata that predates the unconformity.

732

Figure 1
[Click here to download high resolution image](#)



Figure 2

[Click here to download high resolution image](#)

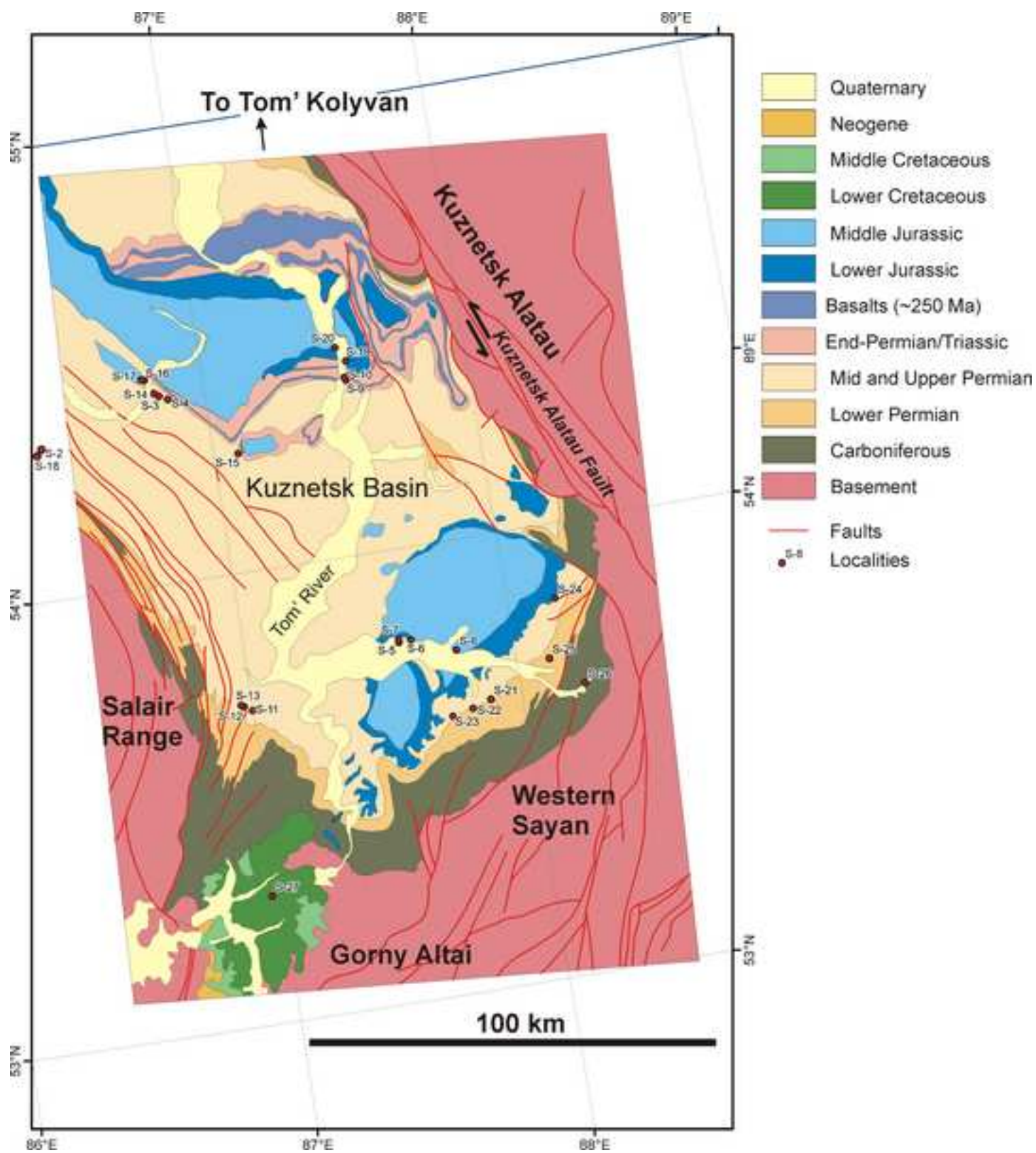


Figure3

[Click here to download high resolution image](#)

Age	Series (Group)	Suite (Formation)	Sub-suite
Lower-Middle Jurassic	Tarbaganskaya	Tersyukskaya	-
		Osinovskaya	-
		Abashevskaya	-
		Raspadskaya	-
Lower-Middle Triassic	Abinskaya	Yaminskaya	-
		Sosnovskaya	-
		Mal'tsevskaya (T ₁ m ₁)	-
Upper Permian	Kol'chuginskaya	Yerunakovskaya (P _{2er})	Tailuganskaya (P _{2t}) Gramoteinskaya (P _{2gr}) Leninskaya (P _{2Ln})
		Il'inskaya (P _{2il})	Uskatskaya (P _{2usk}) Kazankovo-Markinskaya (P _{2k-m})
		Kuznetskaya (P _{1kuz})	-
Lower Permian	Balakhonskaya	Upper Balakhonskaya (P _{1bl})	Usyatskaya (P _{2us}) Kemerovskaya (P _{1km}) Ishanovskaya (P _{1i}) Promezhutochnaya (P _{1pr})
Carboniferous		Lower Balakhonskaya (C _{2-3bl})	Alykaevskaya (C _{2-3al}) Mazurovskaya (C _{2-3mz})
		Ostrogskaya (C ₁ ³ ostr)	-
	“Lower Carboniferous”		

Figure 4

[Click here to download high resolution image](#)

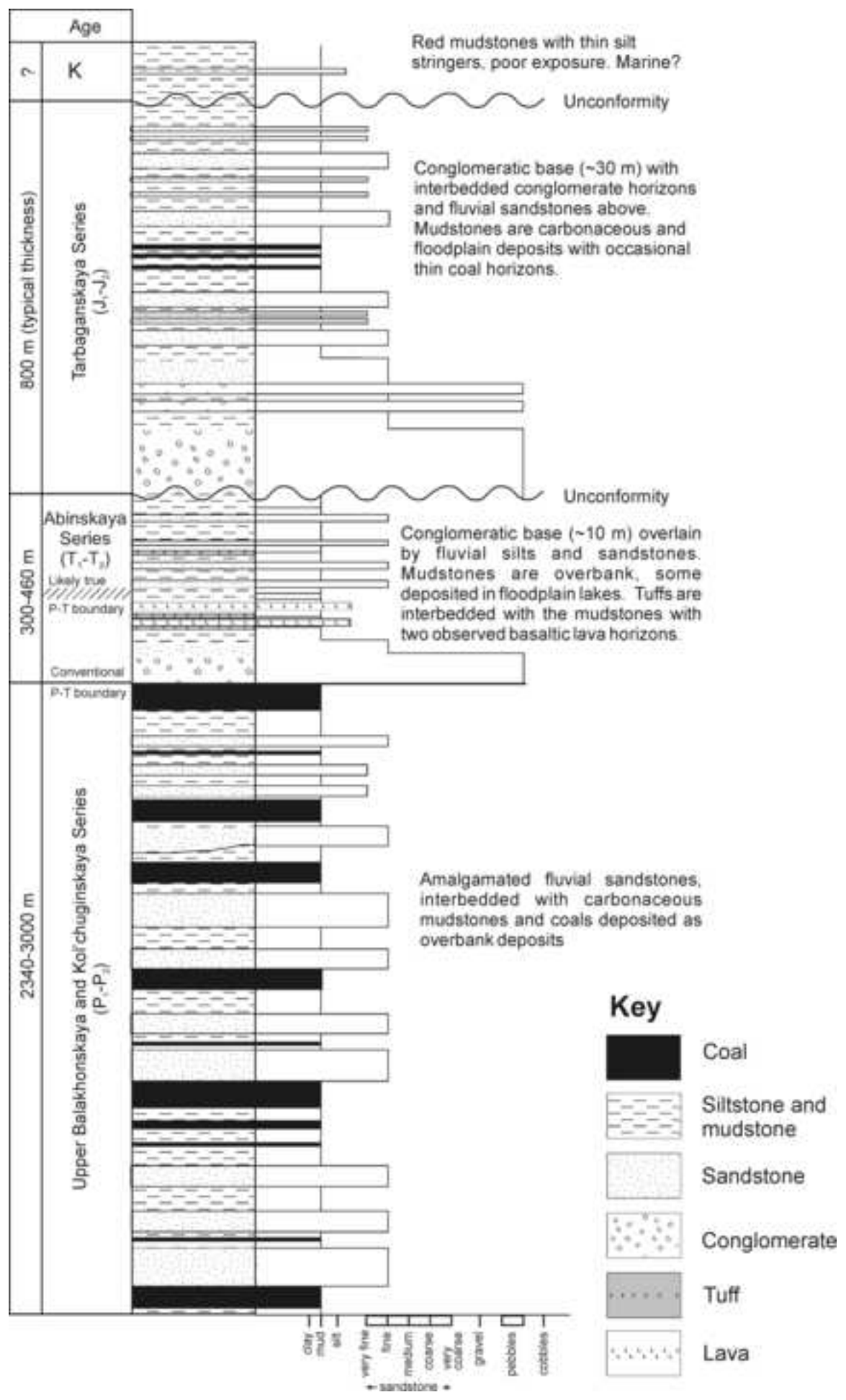
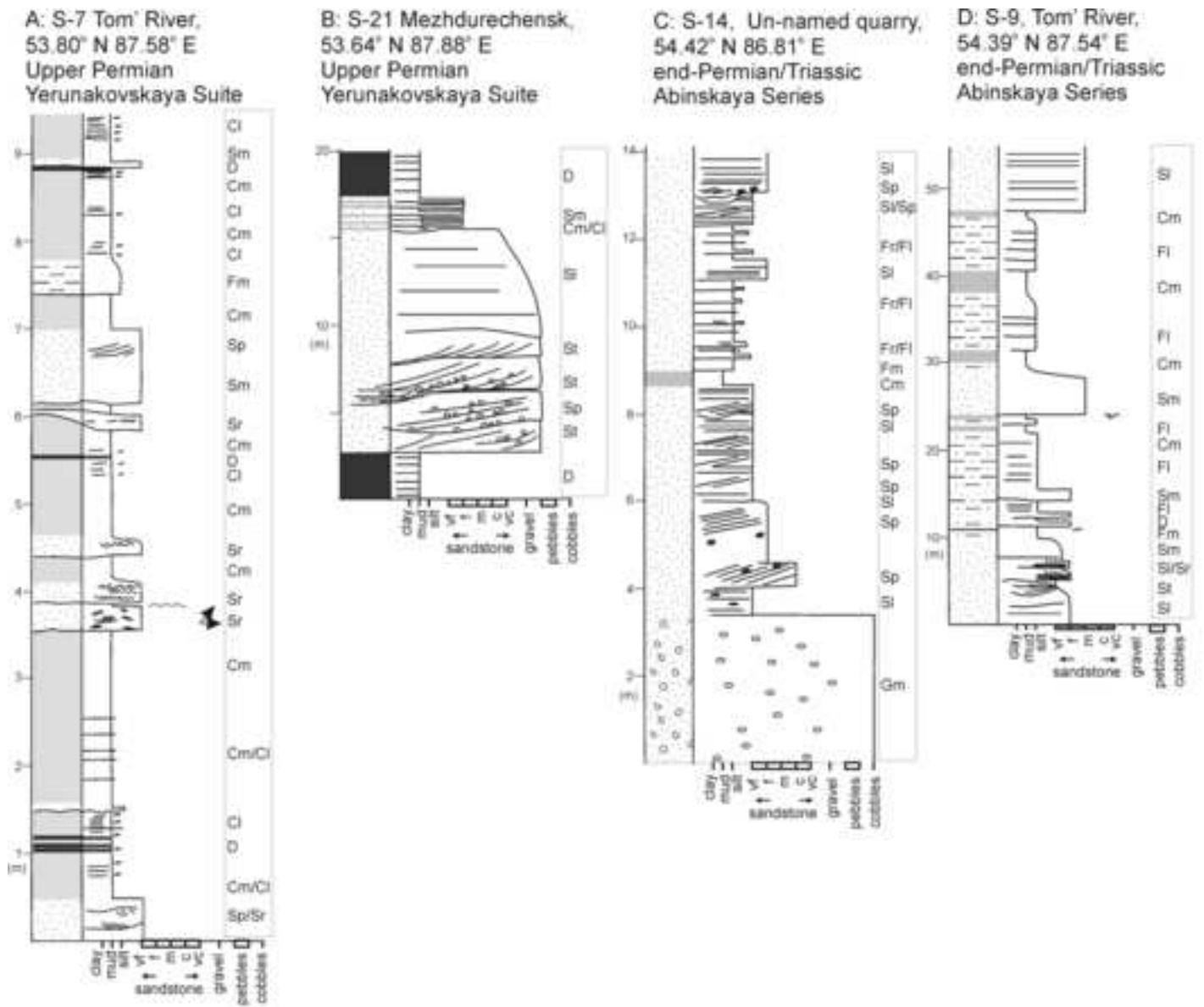


Figure 5
[Click here to download high resolution image](#)



Figure 6A-D

[Click here to download high resolution image](#)



Key
















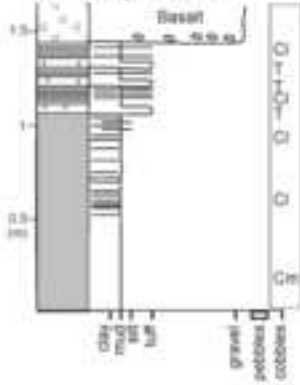
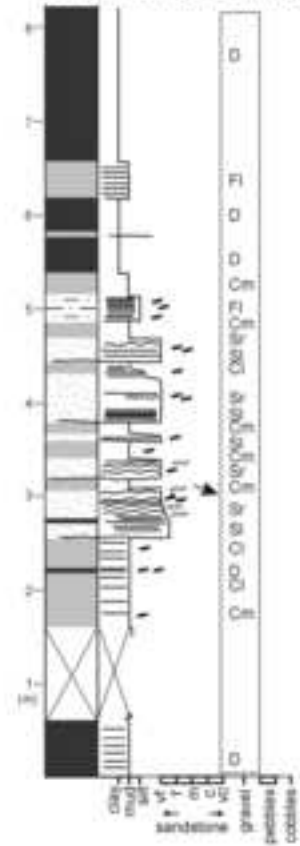
- | | | | | | |
|---|--------------|---|-----------------------------|---|---------------------------------------|
|  | Coal |  | Trough cross-stratification |  | Pebble clasts |
|  | Mudstone |  | Planar cross-stratification |  | Organic fragments (incl. fossil wood) |
|  | Siltstone |  | Ripple cross-lamination |  | Coal clasts |
|  | Sandstone |  | Parallel lamination |  | Flame structure |
|  | Conglomerate | | |  | Palaeocurrent |
|  | Tuff | | | | |

Figure 6E-G
[Click here to download high resolution image](#)

E: S-4 Un-named quarry,
 54.41° N 86.86° E
 end-Permian/Triassic
 Abinskaya Series



G: S-19 Tom' River,
 54.43° N 87.55° E Jurassic



F: S-6 Tom' River,
 53.80° N 87.62° E Jurassic

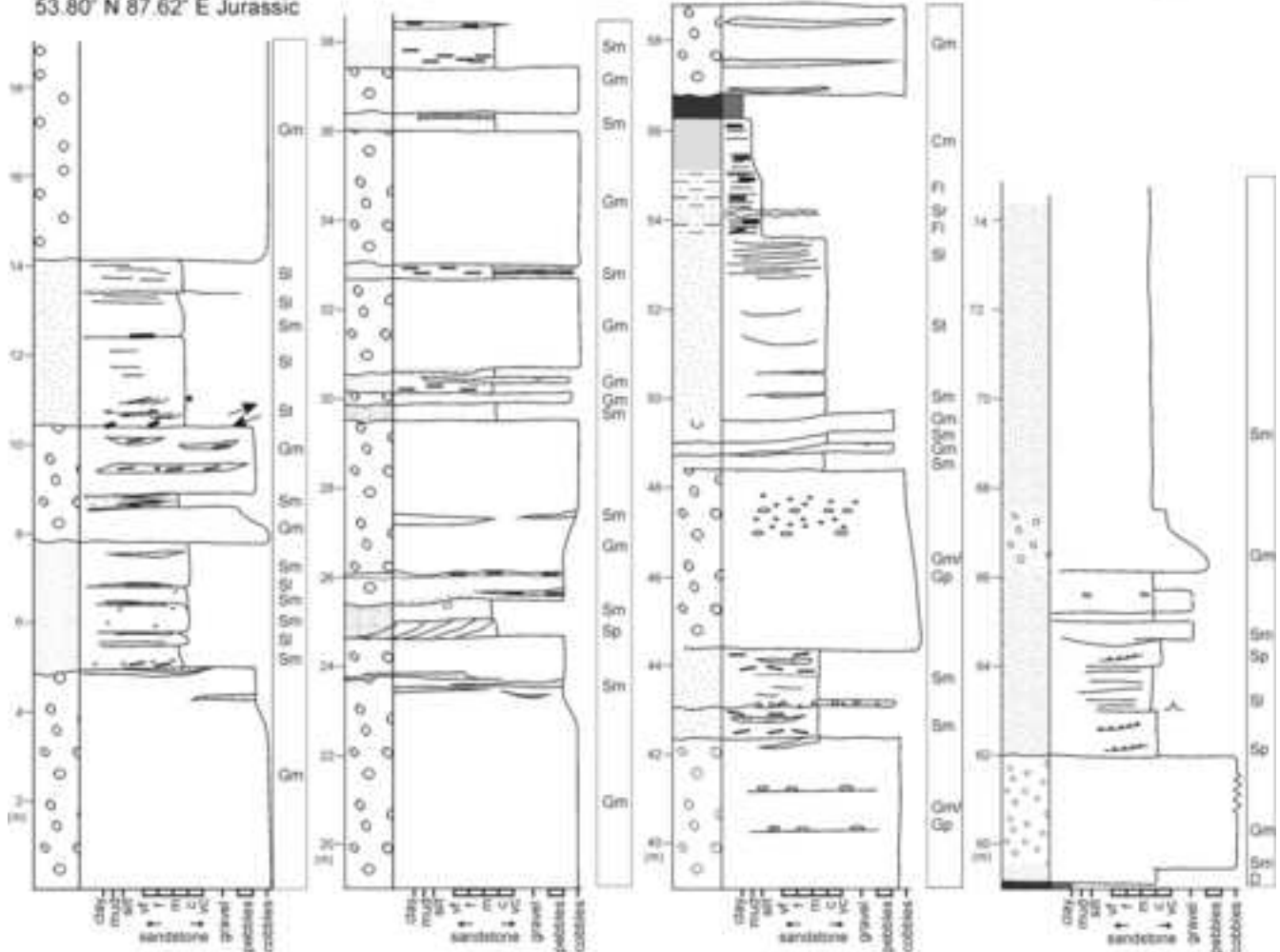


Figure 7
[Click here to download high resolution image](#)

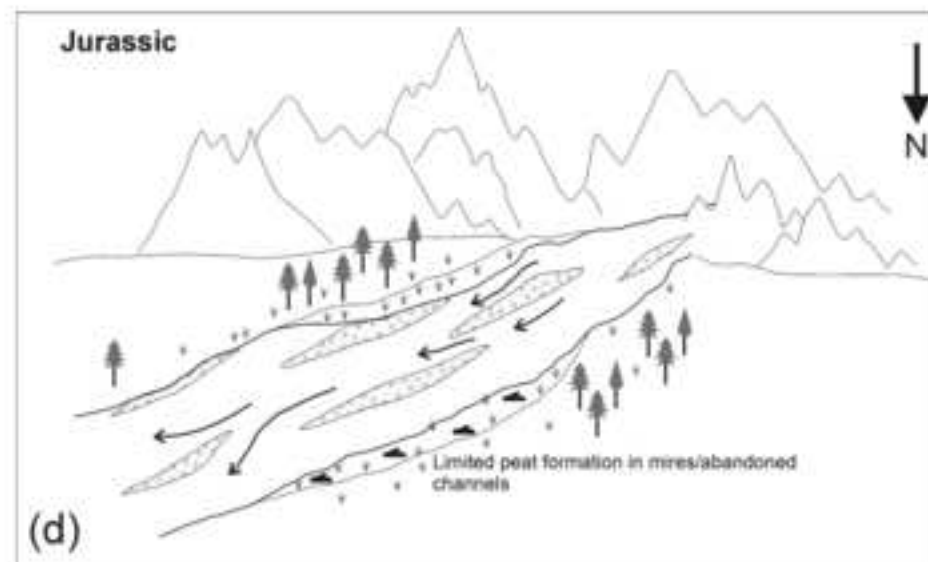
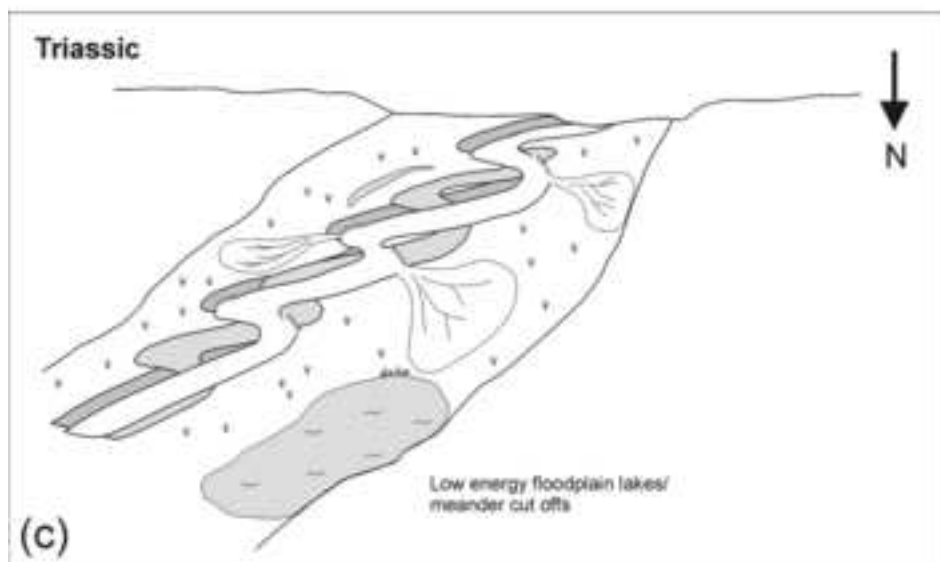
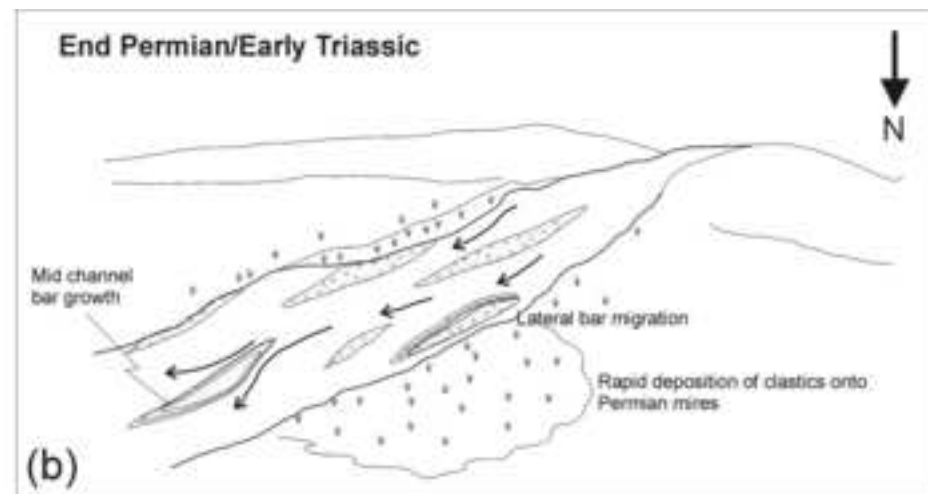
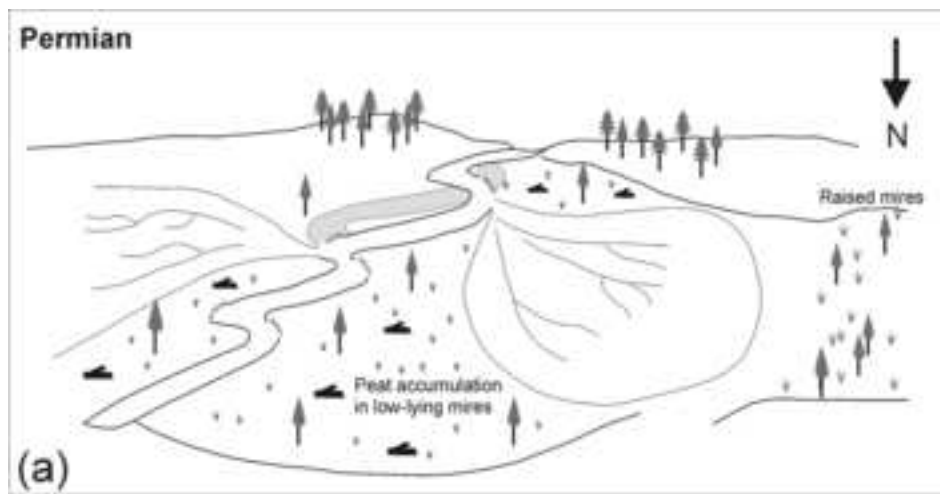
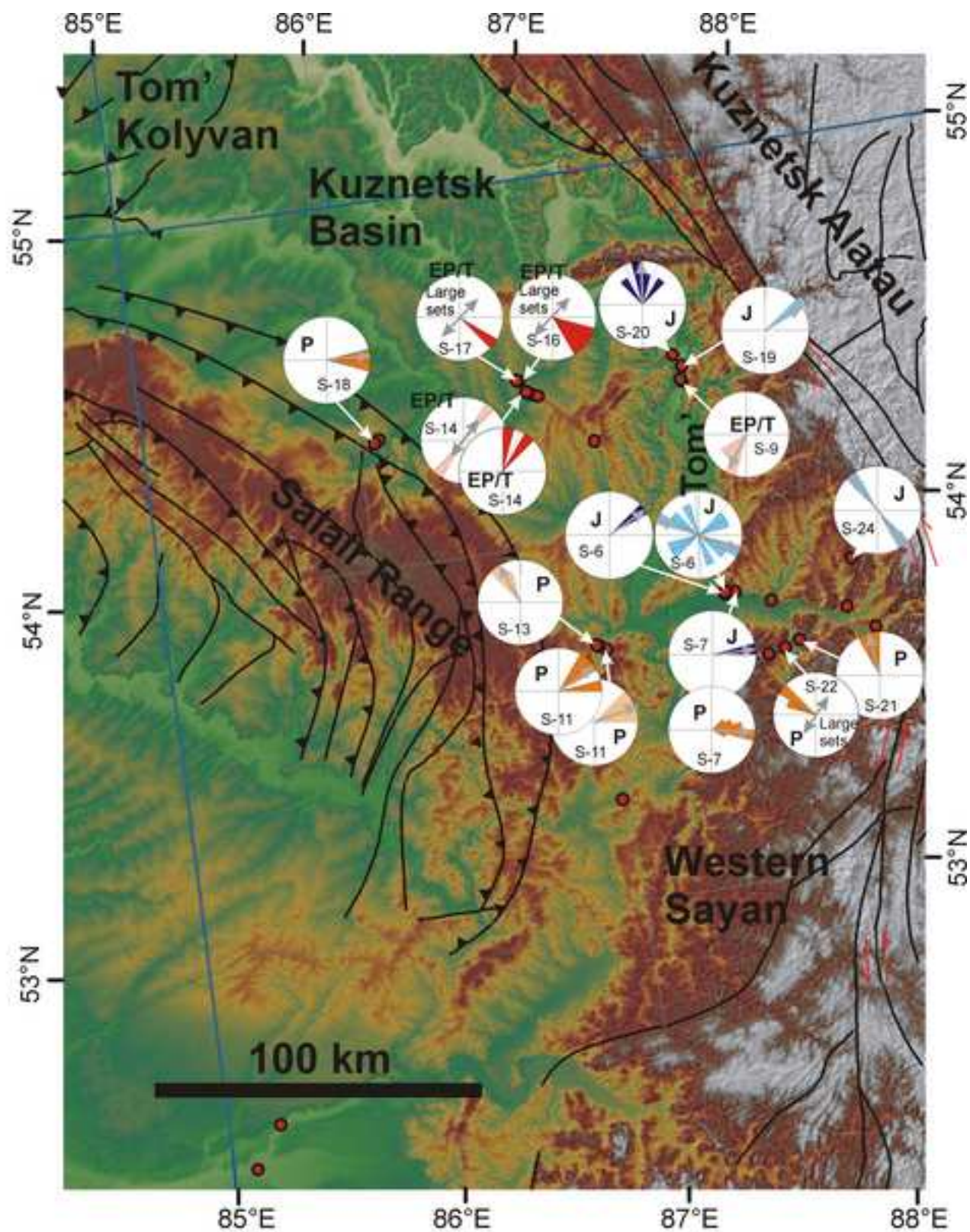


Figure 8

[Click here to download high resolution image](#)



● Localities

Palaeocurrent direction:

dark colour - dune bedforms/large bedform sets
pale colour - ripples/current fabrics

↔ Mean palaeocurrent vectors

P - Permian (Orange)

EP/T - End Permian/Triassic (Red)

J - Jurassic (Blue)

Figure 9

[Click here to download high resolution image](#)



Table 1

[Click here to download Table: Table 1 facies divisions.doc](#)

Table 1: Facies divisions for the Kuznetsk Basin

Lithology	Code	Sedimentary structures	Bioturbation/ palaeoflow	Occurrence	Interpretation
Massive Mudstone	C	Structureless. Colouration varies from red-brown, grey, black.		1-2 cm thick mudstone beds occur between coal seams, both laterally continuous for ~100m. Grey msts grade upwards over 5 cm to become black and carbonaceous with coal layers above.	Suspension fallout from standing bodies of water following overbank flows or from channel abandonment.
Laminated mudstone	Cl	Mudstone with cm-scale parallel laminations, well-cemented to friable. Friable mudstone contains carbonaceous material on laminations. Can consist of paper laminations. Colouration varies from red-brown, grey, black, green.	Green paper laminated mudstones occur with monospecific bivalve casts and mm thick tuffaceous layers.		Suspension fallout from standing bodies of water following overbank flows or from channel abandonment. Carbonaceous material within the mudstone is preferentially aligned along surfaces during deposition, making it laminated. The well-laminated green mudstones with monospecific bivalves suggest deposition within sediment starved, environmentally stressed lacustrine environment.
Coal	D	Structureless and blocky, range in thickness from 1-2cm up to a max thickness of 20m. Large seams are laterally continuous for 100m.	No evidence of rootlets or soil formation, therefore coal may have formed from transported organic material.	1-2 cm thick coal layers occur within mudstones. Thicker coal seams (>2m) contain ~40 cm thick, laterally continuous, mudstones.	Vegetated floodplain areas, some of which were waterlogged (high water table), reducing conditions in floating, low lying or raised mires. Mires are periodically inundated with mudladen floodwater (part of a distal crevasse splay).
Massive Siltstone,	Fm	Structureless siltstone. Beds laterally continuous up to 50m, commonly erosive at base.		Interbedded with mudstone, carbonaceous mudstone and thin coal layers. Often fines upwards into mud-prone intervals.	Deposition by crevasse splay sheetfloods and minor crevasse channel environment in a distal floodplain environment.
Laminated siltstone	Fl	Parallel laminated siltstone. Carbonaceous material and wood fragments drape laminations.		Interbedded with mudstone, carbonaceous mudstone and thin coal layers. Grades from bed parallel lamination to ripple lamination upwards in a bed.	Deposition by crevasse splay sheetfloods and minor crevasse channels in a distal floodplain environment. Parallel lamination indicate decreasing flow velocities due to flow expansion and deceleration away from the main fluvial system.
Ripple cross-stratified siltstone	Fr	Uni-directional ripple cross laminated siltstone with rare climbing ripples. Carbonaceous material and wood fragments drape ripple foresets.	Ripples NW-SE, NE-SW, dominated to the NE and NW.	Interbedded with mudstone, carbonaceous mudstone and thin coal layers. Occur at the top of parallel bedded siltstone intervals.	Deposition by crevasse splay sheetfloods and minor crevasse channels in a distal floodplain environment. Ripple lamination also indicate decreasing flow velocities due to flow expansion and deceleration away from the main fluvial system.
Parallel laminated sandstone	Sl	Unidirectional low angle planar cross-stratified sandstone. Carbonaceous material and wood fragments drape foresets.	Unidirectional flow to east.	Interbedded with mudstone, carbonaceous mudstone and thin coal layers.	Deposition by crevasse splay sheetfloods and minor crevasse channel environment in a distal floodplain environment. Low angle cross-stratification indicate decreasing flow velocities due to flow expansion and deceleration away from the main fluvial system.

Table 1 (continued): Facies divisions for the Kuznetsk Basin

Planar cross stratified sandstone	Sp	Uni-directional, planar cross stratified, v.fine to coarse grained sandstone with normal grading. Cross-set preservation thickness of varies from 0.15-1m up to 6-10 m. (Cm scale coal clasts occur along forests.	0.5-1 m high forsets (Permian?- Loc.S21) & indicate palaeoflow to North. Similar scale forsets at Loc.S18 show palaeoflow to the East. Larger 6-10m forsets show palaeoflow to the NW (Permian?- Loc. S21 & S22). 15-20 cm high sets at S14 show palaeoflow to N-NE.	Mudstone intervals, cm in thickness, are interbedded with this facies.	Intra channel setting of mixed and bedload transported material, possibly within a meandering system. Large in-channel bar forms are preserved.
Trough cross bedded sandstone	St	Uni-directional, trough cross-stratified fine to medium? grained sandstone with common rounded to well rounded pebble grade material (0.2-6 cm in length) forming lags. Silicified and carbonised wood upto 1m in length and 20cm in diameter occur at the base of channels and flakes of carbonised material occur along laminations. Cm scale angular coal clasts at base of beds.	Palaeoflow measurements from wood aligned in channels indicate a flow northwest - southeast and northeast – southwest (S-6).	Pebbles are composed of Quartz, granite, black chert, limestone and sandstone, pink rhyolite, green tuff.	Intra channel setting of mixed and bedload transported material, possibly within a meandering system.
Ripple cross stratified sandstone	Sr	Uni-directional, ripple cross stratified, fine to medium grained sandstone.	Jurassic - Palaeocurrent indicators to the northeast or northwest. Cm scale ripples (Loc. S11, S13) show palaeoflow to the NE and NW respectively.	.	Intra channel to overbank setting of mixed and bedload transported material, possibly within a meandering system.
Massive Sandstones	Sm	Structureless fine-coarse grained sandstone, forming beds up to 5 m in thickness.			Intra channel setting of mixed and bedload transported material, possibly within a meandering system.
Massive Conglomerate	Gm	Massive, matrix to clast supported conglomerate with clasts from gravel to cobble in size.		Up to 10 m thick intervals from multiple events.	Fluvial intra channels setting with bedload transported material in a high energy system.
Planar cross-stratified conglomerate	Gp	Uni-directional, planar cross-stratified coarse, matrix to clast supported conglomerate composed of well-rounded –sub rounded, poor to well sorted gravel to cobble clasts. Rare angular clasts occur. Sets are up to 20 m high (Loc. S16) and clasts range in size from 0.5- 10 cm, max 60cm in length.	Palaeoflow to SE, E at Loc. S16. foresets are seen to abruptly down lap onto coal seams below (Loc 16).	Clasts are grey sandstone, red and black chert, siltstone, mudstone, rhyolite and possibly Basite. Some indication of clast imbrication. Within the conglomerates, decimetre to metre scale channels are infilled with fine to coarse-grained sandstone and are often incised by later events filled with conglomerate deposits.	Fluvial intra channel setting with bedload transported material in a high energy system.
Tuff	T	White, very fine grained sediment, occurs as mm to cm thick laterally continuous horizons.		Tuff layers are interbedded with well laminated green mudstones. Tuff horizons increase in thickness up section (Loc. S4) until a basaltic lava occurs.	Formed by fall out from volcanic eruptions. Likely to be deposited and preserved in a lacustrine environment where reworking did not occur.

Table 2[Click here to download Table: Table 2 Locality information.doc](#)

Locality	Latitude (decimal degrees north)	Longitude (decimal degrees east)	Stratigraphy
S-1	53.79	83.54	modern river
S-2	54.35	86.10	Carboniferous/Permian
S-3	54.42	86.83	modern river
S-4	54.41	86.86	Triassic
S-5	53.79	87.58	Permian/Jurassic
S-6	53.80	87.62	Jurassic
S-7	53.80	87.58	Permian/Jurassic
S-8	53.76	87.78	Jurassic
S-9	54.39	87.54	Triassic
S-10	54.39	87.53	Permian/Triassic - basalt
S-11	53.70	87.00	Permian
S-12	53.71	86.97	Permian
S-13	53.71	86.96	Permian
S-14	54.42	86.81	Permian/Triassic
S-15	54.26	87.09	Triassic
S-16	54.45	86.78	Permian/Triassic
S-17	54.46	86.77	Permian/Triassic
S-18	54.34	86.08	Permian
S-19	54.43	87.55	Jurassic
S-20	54.46	87.52	Jurassic
S-21	53.64	87.88	Permian
S-22	53.62	87.81	Permian
S-23	53.61	87.73	Permian
S-24	53.83	88.18	Permian/Jurassic
S-25	53.71	88.12	Permian
S-26	53.64	88.24	modern river
S-27	53.28	86.97	Cretaceous
S-28	52.42	85.10	modern river
S-29	52.53	85.23	modern river

Table 2: Locality information for this study. Some of these localities are in active open-cast coal mines, such that the outcrop appearance may have changed since this study was carried out.